Progress In Electromagnetics Research B, Vol. 102, 37–60, 2023

A Compact Off-Set Edge Fed Odd-Symmetric Hybrid Fractal Slotted Antenna for UWB and Space Applications

Sanjay Singh[1], Atul Varshney[1], Vipul Sharma[1], Issa Elfergani[2, 3, *], Chemseddine Zebiri[4], and Jonathan Rodriguez[2, 5]

Abstract—This article demonstrates the design development, fabrication, and testing of an off-set edge-fed monopole hybrid fractal antenna for ultra-wideband (UWB) applications at a design frequency of 3.2 GHz. The proposed monopole antenna is compact 38.12 mm × 38.42 mm, slotted, and uses a combination of two numbers of Koch plus Minkowski hybrid fractal technology. Antenna resonates at four frequencies, i.e., quad tuned (3.2 GHz, 4.94 GHz, 7.21 GHz, and 10.10 GHz). The reflection coefficient, $S_{11} < -10$ dB obtained for the excellent UWB fractional bandwidth 119.55% (2.85 GHz to 11.32 GHz) is more than the standard FCC bandwidth (3.1 GHz–10.6 GHz). The antenna has gain 6.73 dBi at 3.49 GHz, 5.91 dBi at 5.52 GHz, 8.26 dBi at 6.81 GHz, and 8.02 dBi at 10 GHz with a maximum radiation efficiency of 89.81%. The main feature of the proposed work is that the antenna is circularly polarized in frequency bands 3.14 GHz–3.30 GHz (Axial ratio: 1.61 dB) and 9.07 GHz–9.45 GHz (Axial ratio: 2 dB) and elsewhere linearly polarized. A total of 16.37% antenna size miniaturization has been achieved with excellent UWB and S_{11} performance. The measured and simulated reflection coefficients are found in good agreement. Therefore, the fabricated and tested antenna is well suitable for Wi-Max (3.3/3.5/5.5 GHz), ISM (5.725–5.875 GHz), WLAN (3.6/4.9/5.0/5.9 GHz), military band applications (radio location, fixed-satellite and mobile-satellite, S-band, C-band, and X-band satellite communications, etc.), aeronautical radio navigation, radio astronomy, ITU-8, Sub-6 GHz band, and Radar applications.

1. INTRODUCTION

Based on the decade bandwidth the antennas are classified into narrow-band, wide-band, ultra-wideband, and super-wideband antennas. The narrow band antennas are defined with a decade bandwidth lower than 500 MHz, having limited applications in wireless communications. The wideband antennas are assumed with frequencies above 500 MHz and have a great number of applications in wireless communications. To cover narrow-band and wideband applications using a single antenna, ultra-wideband (UWB) antennas are designed. The Federal Communications Commission (FCC) has fixed the unlicensed frequency band from 3.1 to 10.6 GHz for UWB in both outdoor and indoor wireless communication systems [1, 2]. The antennas with bandwidth dimension ratio (BDR) greater than 10 fall into the category of super wideband antennas.

Fractal space-filling geometries are most widely used as antennas to cover constrained spaces. Wired and patch antennas have used this idea. Fractal antennas have become famous and popular

Received 23 May 2023, Accepted 10 July 2023, Scheduled 8 August 2023

* Corresponding author: Issa Tamer Elfergani (i.t.e.elfergani@av.it.pt).

[1] ECE Department, FET Gurukula Kangri (Deemed to be) University, Haridwar 249404, Uttarakhand, India. [2] The Instituto de Telecomunicações, Campus Universitário de Santiago, Aveiro 3810-193, Portugal. [3] School of Engineering and Informatics, University of Bradford, Bradford BD7 1DP, UK. [4] Laboratoire d'Electronique de Puissance et Commande Industrielle (LEPCI), Department of Electronics, University of Ferhat Abbas, Sétif -1-, Sétif 19000, Algeria. [5] Faculty of Computing, Engineering and Science, University of South Wales, Pontypridd CF37 1DL, UK.

due to their small size, light weight, and multi-band capability [3, 4]. The snowflake, tree-shaped, star-shaped octagonal structures, Pythagorean tree, Koch Snowflake fractal, fractal polygon embedded with antenna patch, Koch fractal, and analog-periodic square fractal patch, Minkowski fractal, hybrid fractal combinations are most commonly used fractal antenna geometries [5–13].

Several types of research on fractal antennas have been developed. Introduced slot loading provides additional notch bands in a UWB antenna reflection coefficient plot. That causes interference between the UWB system and neighboring narrow bands wireless applications like Wi-MAX (3.3–3.6 GHz), WLAN (5.15–5.82 GHz), C band (3.8–4.2 GHz), and X-band (7.25–8.39 GHz) [14–19]. Abdelaziz et al. have fabricated a compact, inset-fed tri-band dual symmetrically apart inverted T-slotted antenna on a Rogers RT Duroid 5880 substrate. The antenna exhibits a peak gain of 11.72 dBi at 38 GHz for mm-wave applications and 5G services [20]. Liu et al. have demonstrated a coaxially fed, slotted, dual wideband antenna for dual-polarization. Two slots are concentric. One U-slot and one fraction U-slot are placed at the center of the rectangular patch. The antenna provides a peak gain 8.6 dBi at a frequency of 5.2 GHz for both wide bands [21]. Kaur and Sharma presented an inset-fed rectangular-circular slotted antenna on an FR-4 substrate for quad-band operation. The antenna exhibits a peak gain of 11.45 dBi at a frequency of 8.72 GHz. The designed antenna is suitable for S-band, C-band, and X-band applications [22].

Shimizu and Fujimoto have proposed, analyzed, and discussed the performance and operation principles of a printed Inverted-F antenna for dual-band dual-sense circular polarization with the 3 dB-axial ratio for 2.5 GHz band (5.5% fractional bandwidth), and that for 3.5 GHz band is 10.0% bandwidth [23]. Varshney et al. have designed a multiband frequency reconfigurable antenna using PIN diode (BAR-64-02 V) for narrow and wideband functioning [24]. Varshney et al. have used split ring resonator (SRR) triplet to fabricate and analyze an outer fractal-based tri-arm fan-shaped antenna with a gain of 7.13 dBi and fractional bandwidth (FBW) of 48.98%. The outer-fractal technique increases antenna size [25]. Ultra-wideband (UWB) wireless communication is a new method for delivering massive volumes of digital data over a wide frequency spectrum utilizing short-pulse, low-powered radio signals. UWB signals or systems have a relative bandwidth (BW) of more than 20% or an absolute bandwidth greater than 500 MHz. The FCC's 14 February 2002 Report and Order allows unlicensed UWB use at 3.1–10.6 GHz. This optimizes radio bandwidth for high-data-rate personal area network (PAN) wireless connectivity, longer-range, low-data-rate applications, radar, and image systems [26]. Ali et al. have developed a small decagonal UWB monopole antenna with < -10 dB bandwidth 139% (2.3–12.8 GHz), a gain of 1.7–5 dBi, outstanding time-domain characteristics, and average radiation efficiency $> 88\%$. UWB operation requires ground plane truncation [27]. Verma et al. have described an electromagnetic energy harvesting device in the shape of a maple leaf. The antenna has a super-wide band operating frequency range of 5–32 GHz, excellent matching, and a peak gain of 8 dBi at 23 GHz [28]. Swedheetha et al. have proposed an array of 1×3 antennas using a meandered line for impedance matching in power divider side arms, one Minkowski fractal-based antenna, and two inset feed microstrip rectangular patch antennas that cover applications like GSM, WLAN, Wi-MAX, and Cognitive radio services [29]. Wei et al. have provided work to reduce the mutual coupling effect up to -35 dB by utilizing an electromagnetic band gap (EBG) filter and fractalized defective ground in multiple input multiple output (MIMO) systems with the increased number of iterations [30].

Amini et al. have designed a high gain fractal antenna for multi-wideband applications on a Roger RO4003 substrate with permittivity 3.55. The antenna achieves a high gain of 11.15 dBi using log-periodic square fractal [13]. Fonseca et al. have presented an inset-fed dual-slotted using Koch curve third iteration on an FR-4 substrate at 2.4 GHz. The antenna achieves a maximum gain of 5.71 dBi at 5 GHz and quad-wide bands [31]. Sharma and Sharma have presented two hybrid fractal antennas, which supported wideband applications. The first designed antenna has two units of a Koch-Koch hybrid slot in the center of the rectangular patch and a center-fed line that operates at the two broadband frequencies. While the other designed antenna has a single unit of Koch-Minkowski hybrid slot that is placed at the center of the rectangular patch with a quarter-wave transformer — feed line for dual widebands. The two designed antennas attain peak gains of 7.77 dBi and 5.73 dBi, respectively [32]. Tizyi et al. have suggested a coplanar waveguide (CPW) fed small fractal UWB (3.4–16.4 GHz) Koch Snowflake form antenna for the use in radio frequency identification (RFID) applications. This antenna has a gain of more than 5 dBi, a voltage standing wave ratio (VSWR) less than 2, an omnidirectional

radiation pattern, and a constant group delay [33].

Ladhar et al. have proposed an off-set fed random irregular fractal slot created by Cellular-Automata (CA) approach. The patch achieves UWB performance for the full FCC range. Research work does not provide any information related to the time domain group delay analyses for the effectiveness of the proposed approach [34]. Kim and Kim have proposed a dual-polarized broadband microstrip patch antenna for a 5G mm-Wave antenna module. The antenna radiator is a symmetrical structure with L-probes at relative positions. This excites orthogonal resonant modes to enable dual linear polarizations for large MIMO polarization diversity. Characteristic mode analysis (CMA) examined the antenna's operation. A single antenna's bandwidth was 23.1% (23.29 GHz), and a gain of 5 dBi, and single antenna cross-polarization suppression was 15–20 dB [35].

Motivation of Research: As mentioned in the above paragraphs, Fonseca et al. have designed and fabricated an antenna using a vertically symmetrical single-unit Koch curve with iteration three. This results in quad narrow bands with a peak gain 5.71 dBi at a frequency of 2.37 GHz [31]. On the other hand, Sharma and Sharma fabricated two different antennas. One uses two units of Koch-Koch curves in the middle about the width of the antenna patch, and the other slotted antenna is designed using a hybrid combination of the one unit of Koch and one unit of Minkowski curves in the middle of the patch along the patch width [32]. All the designed antennas are linearly polarized. One uses edge feed, and the other two use quarter-wave transformer feeding techniques. All these antennas result in a narrow bandwidth and multi-band antennas. The antenna in [31] is symmetric around the patch length while Reference [32] antennas are symmetric around the patch width. The research gap of these antennas motivates us to make a novel fractal shape with different kinds of feeding techniques to achieve circular polarization. Another motivation of the present study is to achieve UWB performance instead of multi-narrow bands. This research gap motivates authors to make a slot that is a hybrid combination of the two or more units of the Koch as well as the Minkowski curves, asymmetrically placed along the width and shifted along the length. To achieve the linear as well as the circular polarization, an off-set feeding technique is utilized in the proposed design. The complete ground is reduced to achieve wideband performance or to achieve ultra-wideband performance. Moreover, the already-designed antennas utilize symmetrical slots and or a combination of single units of the fractal curves.

Research Objectives: The research gaps in the existing literature are fulfilled by considering the following research objectives;

- The primary aim (novelty) of this proposed work is to obtain a new hybrid fractal slotted antenna geometry, using two units of Koch and two units of Minkowski curves hybrid combinations [31, 32].
- Another objective of this research is to use a filleted corner reduced ground structure to achieve a monopole antenna and UWB performance [26, 31].
- Furthermore, the present work plans to apply rarely used off-set feeding to obtain circular polarization along with linear polarization [15, 35].
- One of the major intents of the proposed work is to use a combination of off-set feeding along with odd-symmetric hybrid slotted (a rare combination of two units of Minkowski and two units of Koch fractal odd-symmetric) structures to achieve the UWB performance and dual polarization [15, 31, 35].

This article proposes an off-set fed odd-symmetric monopole fractal antenna for UWB applications. The proposed antenna is derived from a conventional rectangular monopole antenna. To achieve wide bandwidth and good impedance matching, a conventional rectangular monopole antenna has been modified by adjoining a pair of Koch-Minkowski hybrid slots at the top layer of the patch and also by modifying its partial ground plane. The novelty in the structure is brought by introducing two mixed odd-symmetric hybrid Koch-Minkowski fractal slots within the patch which facilitates extending the -10 dB bandwidth. The introduced slot helps to increase the current path electrical length and thus keeps the dimensions of the antenna unharmed. Two significant contributions of the presented paper are: A filleted ground plane, along with reduced length, is employed to minimize the effect of cloud capacitance at the corner, which in turn is used to nullify the inductive effect of patch ensuing in an improved impedance matching. Drawing the most attention for the proposed radiator is its medium BDR (718) and its -10 dB ultra-wide bandwidth (2.11–11.73 GHz), which is attained by augmenting the electrical length of the patch with fractional bandwidth of 119.58% and bandwidth ratio of 5.56 : 1. In

this paper, all the frequency domain characteristics in terms of radiation patterns, reflection coefficient, axial ratio, radiation efficiency, and gain are investigated to estimate antenna performance.

The paper is organized as follows. Section 1 describes the research background literature and the main objectives of the proposed research work. Section 2 explains the antenna design structure development and parametric studies. Section 3 presents the comparisons of the simulated and measured results with the state-of-the-art. The work is concluded with the proposed design utilization and their future scope.

2. MATERIALS AND METHODS

2.1. Development of Hybrid Curve

The proposed antenna hybrid fractal is developed from the addition of two units of inverted Minkowski-Minkowski curves and two units of inverted odd-symmetric Koch-Koch curves as illustrated in Figure 1.

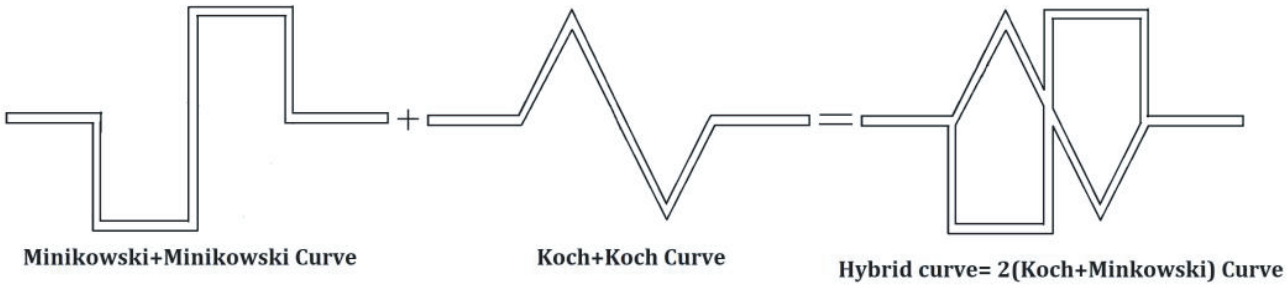

Figure 1. Hybrid Koch-Minkowski curve.

2.2. Antenna Design Structure Development with Hybrid Fractal Curve

A compact (38.12 mm × 38.42 mm × 1.6 mm) hybrid fractal slotted (as shown in Figure 1) ultra-wideband (UWB) antenna is fabricated on a low-profile 1.6 mm thick FR-4 substrate with relative permittivity 4.4 and loss tangent ($\tan\delta = 0.02$). FR-4 substrate is most widely used up to frequencies lower than 10 GHz [22]. Although using low-cost substrate antenna designs is also available for frequency range lower than 10 GHz, FR-4 substrate shows non-linear variation in permittivity with increase in frequency and hence becomes unstable [35]. The λ_0 value is evaluated as 93.75 mm, and the main concern (feature) of this paper is to miniaturize the size of the antenna and to achieve ultra-wideband performance. The dual polarizations and multi-tuning frequencies are additional features of the proposed design antenna. The proposed design achieves a UWB performance below −10 dB reflection coefficient value (2.85 GHz-to-11.32 GHz) more than the FCC's 2002 well-defined UWB range (3.5 GHz–10.6 GHz) [26]. An ANSYS Electronic Desktop Terminal (EDT), HFSS 2022 has been used for the analysis and computation of the proposed antenna design. The proposed antenna has been designed at a frequency of 3.20 GHz. The width and length of initially calculated microstrip rectangular patch at this design frequency were 28.52 mm and 21.92 mm [32]. Finally, these values are optimized to 22.6 mm and 21 mm respectively to achieve better resultant performance parameters. The antenna was excited with a 50 Ω center edge fed line (Ant. 1 of Figure 2). Then a hybrid double Koch-Minkowski curve of width 'a' 0.5 mm is introduced in Ant. 1 (Ant. 2 of Figure 2). After that the effect of reduction of ground length (Partial ground plane 'PGP') and off-set was developed and simulated for their optimum length and off-set edge fed location value as depicted in Figure 2 (Ant. 3 and Ant. 4). Further, monopole hybrid fractal slotted antenna for the optimized length of PGP 9.8 mm and off-set 1.74 mm from the middle of the width is simulated, and dual wideband nature (2.73–5.50 GHz and 5.69–10.08 GHz) are obtained (Ant. 5 Figure 2). Finally, filleted corners of the ground of radius 5.0 mm were introduced at the PGP inner ground corners to achieve the single UWB (2.85 GHz–11.32 GHz) of the proposed antenna design structure as depicted in Ant. 6 of Figure 2. All the dimensions of the hybrid fractal slot ('a'-to-'z') and the proposed designed antenna structure are shown in Figure 3(a) and Figure 3(b),

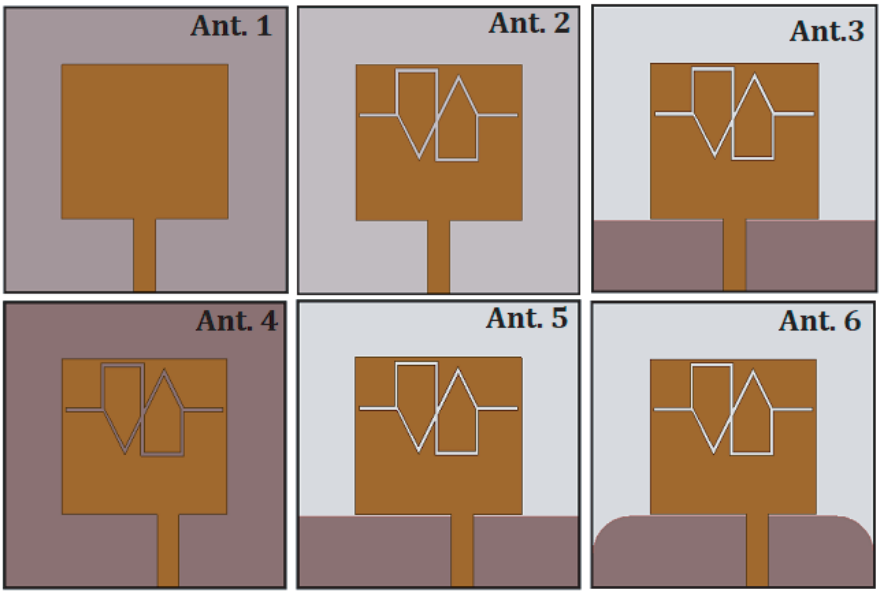

Figure 2. Antenna design development.

Table 1. Dimensions of the slotted hybrid fractal antenna.

Parameter	W_{Sub}	L_{Sub}	W_P	L_P	W_f	L_f	W_{gnd}	L_{gnd}	h	r_{Fillet}
Dimension (mm)	38.12	38.42	22.60	21	3.0	9.8	32.12	9.5	1.6	5.0
Parameter	a	b	c	d	e	f	g	h (slot)	i	j
Dimension (mm)	0.5	5.14	6.57	4.90	4.50	5.88	6	5.38	0.5	5.38
Parameter	k	l	m	n	o	p	q	R	s	t
Dimension (mm)	6.015	6.015	6.06	5.88	6.06	4.88	6.07	4.90	6.56	5.0
Parameter	u	v	w	x	y	z	L_1	L_2	L_3	
Dimension (mm)	5.56	5.165	6.015	5.0	5.0	5.76	6.56	6.58	0.54	

respectively, and measurements of the dimensions in mm are provided in Table 1. A trimetric view of the off-set fed hybrid double Koch-Minkowski slotted fractal antenna with global reference system of space variables is showcased in Figure 3(c).

2.3. Effect of Ground on Hybrid Fractal Slotted Antenna

When the top surface of the rectangular patch is etched by a hybrid fractal slot with the full bottom surface of the substrate covered with the ground conductor, then the slotted microstrip antenna behaves like a multi-tuned narrow band antenna. The length of the ground plane is reduced near the feed without changing the width of the ground surface, then the antenna becomes monopole, and the antenna becomes dual-bands. The filleting of the two inner corners of the antenna results in the UWB. The effect of the complete ground plane (Microstrip antenna), partial ground plane (PGP) with reduced ground length (monopole antenna), and filleted ground plane (rounded corner PGP) on hybrid fractal slotted antenna reflection coefficients are displayed in Figure 4, and their corresponding effects of change in ground length and fillet corner ground are summarized in Table 2.

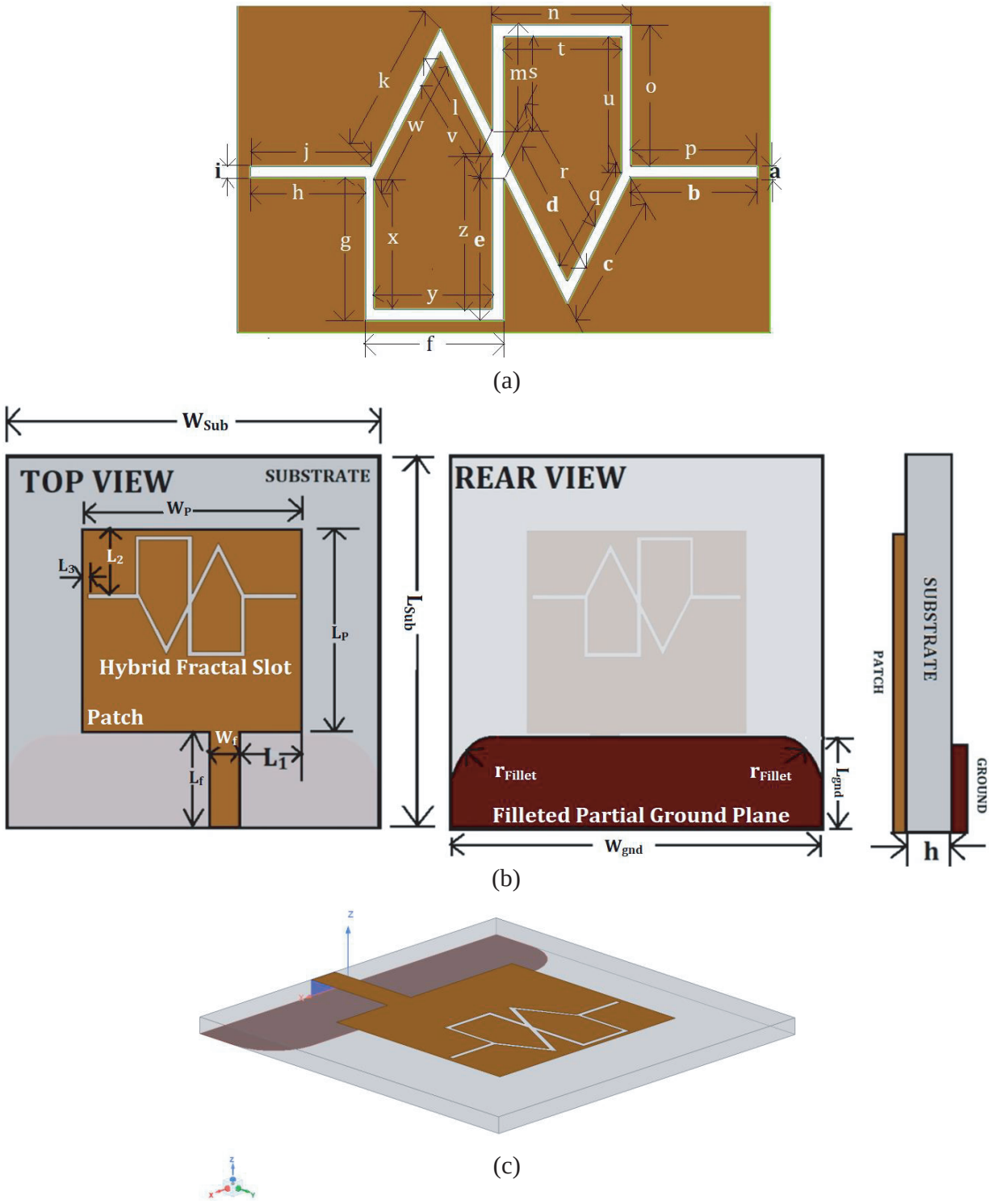

Figure 3. Hybrid fractal slotted antenna geometry. (a) Hybrid fractal slot dimensions designation. (b) Design structure. (c) Hybrid fractal antenna showing global reference system.

2.4. Effect of Hybrid Fractal Slot on Designed Antenna

In the first step, the monopole rectangular antenna is simulated with an odd symmetric Koch-Koch slot. Its reflection plot is dual bands (one narrow band and the other wide band) with multiple-tuning

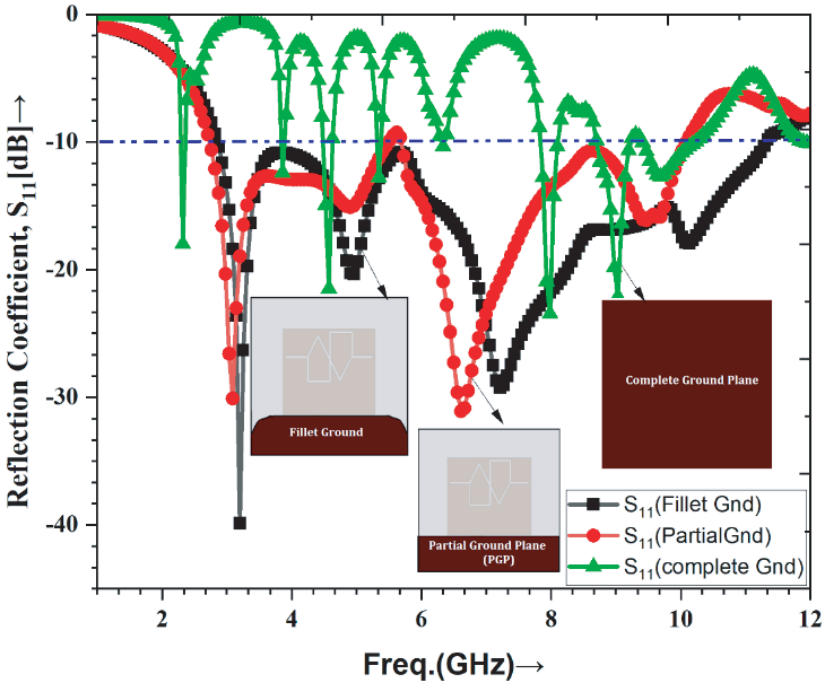

Figure 4. Effect of ground on the hybrid fractal slotted antenna.

Table 2. Substrate width variations.

Ground Shape	Res. Freq. (GHz)	Ref. Coeff., S_{11} (dB)	−10 dB BW, %FBW (GHz)	Antenna Nature
Complete Ground	2.32 3.86 4.57 5.35 6.33 7.99 9.03 9.69	−17.97, −12.32, −21.40, −12.68 −10.34 −23.37 −22.08 −12.69	2.29–2.36 3.84–3.89 4.48–4.67 5.32–5.35 6.31–6.35 7.84–8.10 8.70–9.23 9.41–10.23	Multi-band (octal tuned)
Partial Ground Plane (PGP)	3.10, 4.94 6.63, 9.47	−29.90, −15.09 −30.99, −16.13	2.73–5.50 5.69–10.08	Dual wide band Quad tuned
Fillet Ground	3.20, 4.94, 7.22, 10.12	−39.85, −20.32, −29.19, −17.91	2.85–11.32	UWB band Quad tuned

frequencies. The reflection coefficient plot with an odd symmetric Minkowski-Minkowski slot possesses multi-tuned UWB behavior. In the next step, the monopole antenna is etched with an odd symmetric Koch-Minkowski slot. This slot changes the reflection coefficient plot into a dual wideband by the fillet corner of the PGP [10]; this results in excellent UWB bandwidth. The reflection coefficients plot with all slots is represented in Figure 5, and their recorded resultant parameters are arranged in Table 3.

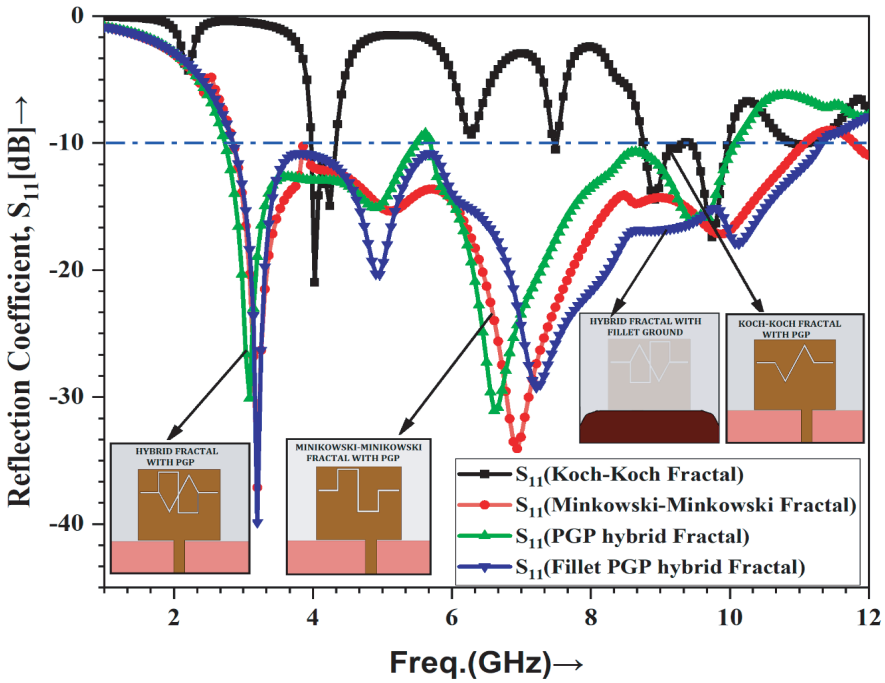

Figure 5. Effect of a slotted fractal on reflection coefficient plots.

Table 3. Effect of the slotted fractal.

Ground Shape	Res. Freq. (GHz)	Ref. Coeff., S_{11} (dB)	−10 dB BW, %FBW (GHz)	Antenna band Behavior
Monopole Koch-Koch fractal	2.81 3.40, 5.08, 7.26, 10.40	−15.02 −16.92, −17.76, −28.48, −16.77	(2.68–2.91) (3.13–11.79)	Dual-band multi-tuned
Monopole Minkowski-Minkowski fractal	3.20, 5.16, 6.95, 9.92	−36.34, −15.31, −33.86, −17.11	(2.85–11.09)	UWB band, Multi-tuned
Monopole Hybrid fractal	3.10, 4.94 6.63, 9.47	−29.90, −15.09 −30.99, −16.13	(2.73–5.50) (5.69–10.08)	Dual wide band Quad tuned
Filleted Monopole hybrid fractal	3.20, 4.94, 7.22, 10.12	−39.85, −20.32, −29.19, −17.91	(2.85–11.32)	UWB band Quad tuned

2.5. Off-Set Feeding Principle or Off-Set Feeding Effect on UWB Antenna Response

The electrical length appending through the hybrid slot side of the rectangular patch must affect the current distribution and electric field that may result in frequency variations from the lower side 2.85 GHz (higher electrical length) and 11.32 GHz (lower electrical length) corresponding to current variations across the hybrid slot.

Off-Set Feeding Principle: There are many feeding techniques in microstrip antenna design like coaxial feed, center edge feed, inset feed, proximity feed, and off-set feeding. The center-edge feeding,

inset feeding, and coaxial feeding are the most widely used by researchers, and literature is also available on these techniques [24]. The proximity feeding technique increases the height of the antenna and is often used. In center-edge feed and inset feed techniques, the current and electric fields are evenly divided and cancel out to each other at the vertical edges. Therefore, only the top and bottom edges of the patch will radiate, and only linearly polarized antennae are obtained. Perhaps by using off-set feeding techniques the current is not evenly divided and results in some amount of radiation because of the difference amount of current and electric field at the side edges of the patch. This will enhance the radiation of the antenna along with the top and bottom edges of the antenna and result in dual polarizations (linear and circular) simultaneously.

Using basic design equations of [31], a center edge-fed rectangular patch antenna is designed. It does not have any transmission of power since the reflection coefficient, S_{11}, is > -1.50 dB. Then the feed is shifted from the center location towards the right by 1.74 mm. This results in five narrow-band resonance frequencies. It is noticed that the center edge feed does not provide any S_{11} value < -10 dB. The Koch-Minkowski slotted rectangular patch off-set fed antenna with full ground gives eight narrow band tuning frequencies. Monopole off-set fed fractal antenna results in two widebands. Finally, filleted ground monopole hybrid fractal slotted antenna results in a UWB reflection coefficient below -10 dB. All off-set fed cases are compared in Figure 6 and well arranged in Table 4.

Table 4. Effect of off-set edge fed on center edge fed hybrid fractal slotted antenna.

Antenna Type	**Edge feeding Technique**	**Res. Freq. (GHz)**	**Reflection Coefficient, S_{11} (dB)**	**-10 dB BW, %FBW (GHz)**	**Antenna Nature**
Microstrip Patch Antenna (MPA)	Center Fed	Nil	> -1.50	Nil	Nil
	Off-set Fed	4.59 6.50 7.12 10.14 11.40	-14.15 -17.26 -29.22 -20.52 -18.37	4.54–4.66 6.35–6.64 6.91–7.34 9.60–10.32 11.18–11.72	Penta Narrow Band
Microstrip Hybrid Fractal Antenna	Center Fed	Nil	> -2.25	Nil	Nil
	Off-set Fed	2.32 3.86 4.57 5.35 6.33 7.99 9.03 9.69	-17.97, -12.32, -21.40, -12.68 -10.34 -23.37 -22.08 -12.69	2.29–2.36 3.84–3.89 4.48–4.67 5.32–5.35 6.31–6.35 7.84–8.10 8.70–9.23 9.41–10.23	Multi-band (Multi-tuned)
Monopole Hybrid Fractal Antenna	Center Fed	Nil	> -2.08	Nil	Nil
	Off-set Fed	3.10, 4.94 6.63, 9.47	-29.90, -15.09 -30.99, -16.13	(2.73–5.50) (5.69–10.08)	Dual wide band Quad tuned
Filleted ground Hybrid Fractal Antenna	Center Fed	Nil	> -2.0	Nil	Nil
	Off-set Fed	3.20, 4.94, 7.22, 10.12	-39.85, -20.32, -29.19, -17.91	(2.85–11.32)	UWB band Quad tuned

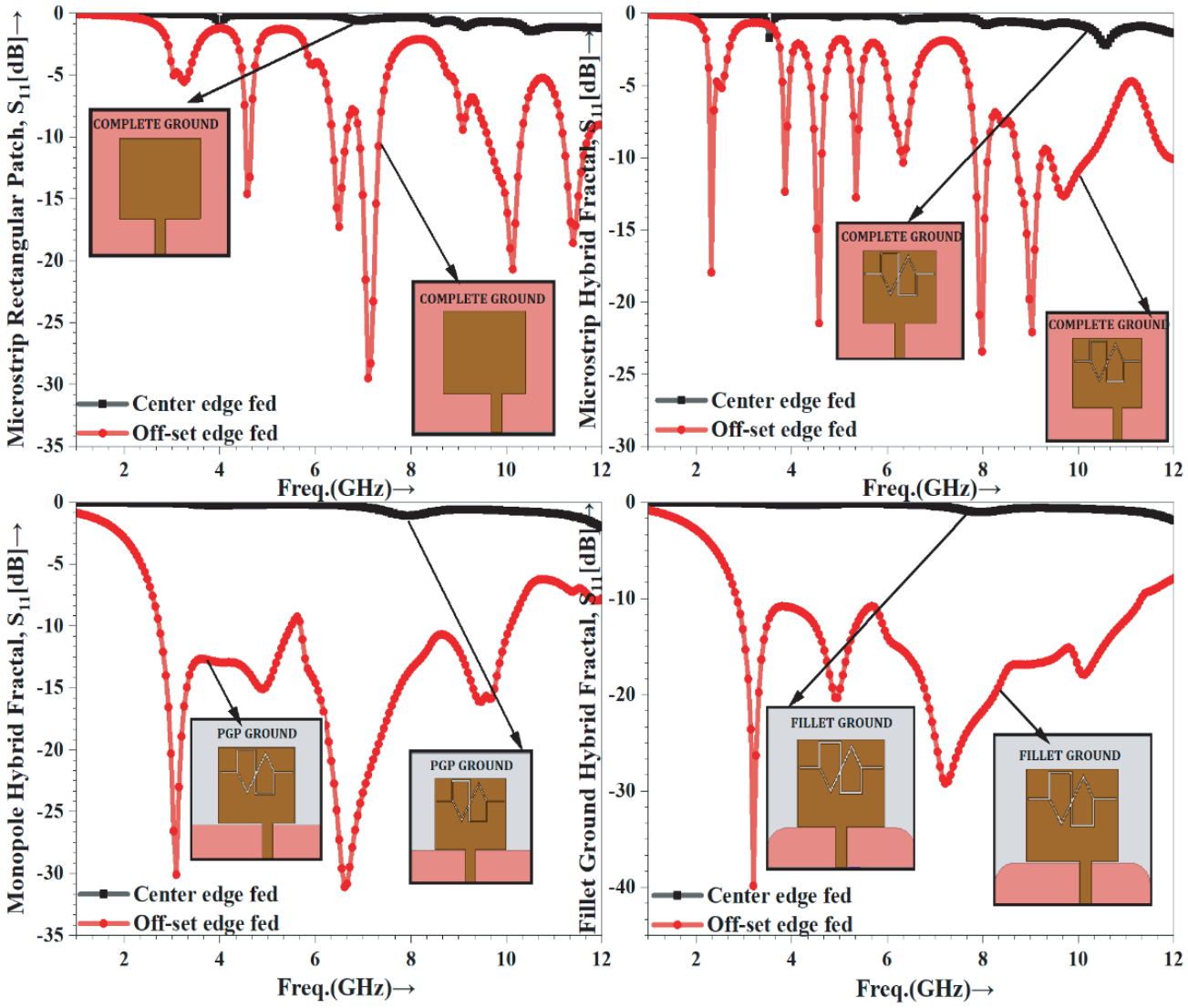

Figure 6. Effect of off-set fed and center edge fed on reflection coefficient plot.

3. RESULTS AND DISCUSSIONS

3.1. Resultant Parameters of Hybrid Fractal Slotted Antenna

The designed antenna with optimized dimensions using photolithography, UV-exposing, and chemical etching process is fabricated on a 1.6 mm thick low profile FR-4 epoxy substrate piece of dimensions 38.12 mm×38.12 mm. The front and rear views of proposed fabricated antenna prototype are represented in Figures 7(a)–(b). The fabricated antenna is tested for reflection coefficient validations on the Agilent N 5247A vector network analyzer (Figure 7(c)). The measured reflection coefficient S_{11} has a −10 dB fractional bandwidth (FBW) of 139% for a frequency range from 2.11 GHz to 11.73 GHz. The measured reflection coefficient curve has four resonant frequencies in the UWB at 2.825 GHz, 4.365 GHz, 6.29 GHz, and 10.91 GHz with S_{11} values −40.97 dB, −17.73 dB, −27.87 dB, and −19.33 dB, respectively. The measured FBW is approximately 20% higher than the simulated FBW (2.85–11.32 GHz). The first three resonant frequencies are deviated a little left (by 0.35 GHz, 0.575 GHz, and 0.93 GHz) from the simulated resonant frequencies 3.20 GHz, 4.94 GHz, 7.22 GHz, and the fourth resonance frequency is deviated right by 0.79 GHz as depicted in Figure 8(a) and illustrated in Table 5. The entire antenna

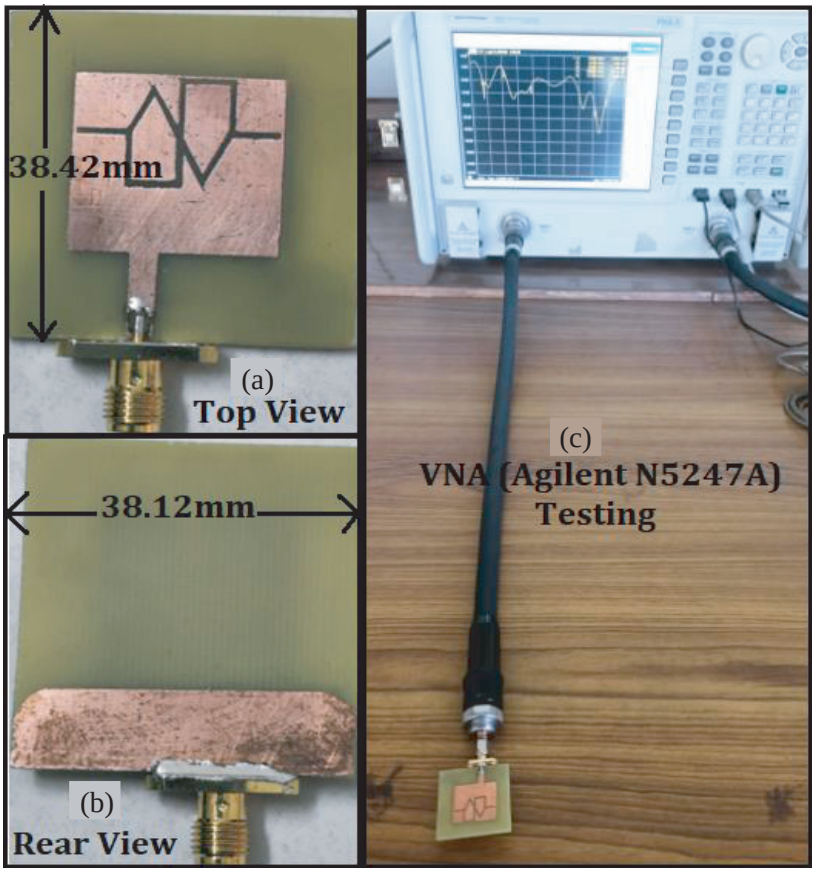

Figure 7. Prototype of the hybrid fractal slotted. (a) Top view. (b) Rear view. (c) VNA testing.

resultant performance parameters are displayed in Table 6. Antenna resonance frequencies not only depend upon the impedance matched but also depend upon the points where the impedance is not properly matched perhaps the reflection coefficient plot, and (S_{11}) values are well below -10 dB level as represented in Figure 8(b). The proper impedance match frequencies correspond to the points where the real part of the impedance is close to $50\,\Omega$ whereas the imaginary part of the impedance is close to zero. These result in the lowest deep in the S_{11} plot values. These resonance frequencies (3.20 GHz, 4.94 GHz, 7.22 GHz, and 10.12 GHz) are represented by blue lines in the plot. The non-impedance matched frequencies are corresponding to the antenna impedance plot containing real as well as imaginary part and provide the non-impedance matching while the reflection coefficient S_{11} plot is lower than -10 dB level which determines the additional resonance frequencies (6.0 GHz, 8.65 GHz, and 9.8 GHz). The blue vertical line represents the resonating frequencies while the green color vertical lines represents the non-resonating frequencies in the graph of Figure 8(b). It is concluded from Figure 8(b) that in [32] the authors used the quarter wave impedance transformer feeding technique which provides excellent impedance matching, which will have closer results to the software-simulated resonant frequencies. In the proposed antenna an off-set feeding technique is utilized which yields some differences in the impedance matching, and this will result in shifts in the resonant frequencies. In the measured reflection coefficient plot, the shape of the curve follows the shape of the simulated reflection coefficient curve with small deviations in the resonant frequencies.

3.2. Gain and Radiation Efficiency Plots of Hybrid Fractal Slotted Antenna

The gain and radiation efficiency of the odd symmetric hybrid Koch-Minkowski slotted antenna at the designed frequency 3.20 GHz are 4.72 dBi and 89.81%, respectively. The proposed antenna gain and

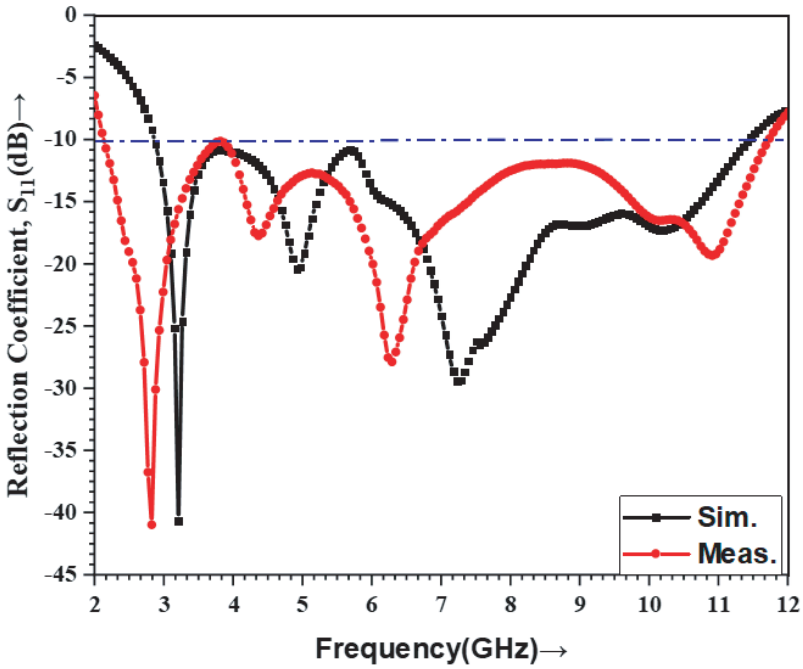

(a)

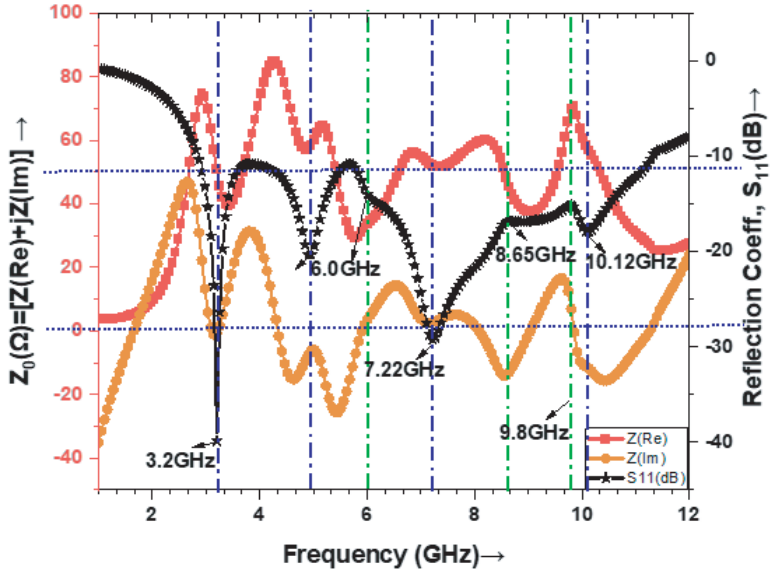

(b)

Figure 8. (a) Simulated and measured reflection coefficient, S_{11} plots. (b) Tuning-frequency of antenna based on impedance matched.

radiation efficiency plots are displayed in Figure 9. The average radiation efficiency of the designed antenna is higher than 85%. The highest value of radiation efficiency 99.97% is obtained at 3.75 GHz. The maximum gain of the antenna is 8.26 dBi at a frequency of 6.83 GHz.

3.3. Axial Ratio and Antenna Polarization of Hybrid Fractal Slotted Antenna

The proposed antenna is dual polarized, i.e., circularly as well as linearly. The antenna is circularly polarized since AR < -3 dB for the frequency bands 3.14–3.30 GHz and 9.07–9.45 GHz and linearly polarized since AR > -10 dB for the bands 1.0–2.86 GHz, 3.48–4.80 GHz, 5.36–6.05 GHz, and 6.91–

Table 5. Simulated and measured results of the proposed hybrid fractal slotted antenna.

Antenna	Res. Freq., f_r (GHz)	Ref. Coeff., S_{11} [dB]	BW (GHz)	FBW (%)	VSWR	Gain (dBi)
Simulated	3.20/ 4.94/ 7.22/ 10.12	−39.85/ −20.94/ −29.19/ −17.91	2.85–11.32	119.54	1.06 @3.23 GHz	4.72 @3.20 GHz
Measured	2.825/ 4.365/ 6.29/ 10.91	−40.97/ −17.73/ −27.87/ −19.33	2.11–11.73	139	1.10 @3.23 GHz	5.01 @3.20 GHz

Table 6. Result of the proposed hybrid fractal slotted antenna.

Antenna Parameter	Simulated Results Values
Resonant frequencies (GHz)	3.20/4.94/7.22/10.12
Reflection Coefficient, S_{11} (dB)	−39.85 at 3.20 GHz, −20.94 at 4.94 GHz, −29.19 at 7.22 GHz, −17.91 at 10.12 GHz
Bandwidth (GHz)	2.85–11.32
Fractional Bandwidth (FBW)	119.548%
Gain (dBi)	7.43 at 1 GHz/6.72 at 3.50 GHz/5.22 at 4.60 GHz/ 5.91 at 5.52 GHz/8.26 at 6.83 GHz/8.02 at 10.02 GHz 9.45 at 12 GHz
Gain at the Design frequency	4.72 dBi at 3.20 GHz
Directivity	5.18 dBi at 3.20 GHz
Radiation Efficiency	89.81%
VSWR	< 1.81 for 2.89–11.22 GHz/1.06 at 3.23 GHz
Axial Ratio (AR)	< -3 dB (3.14–3.30 GHz and 9.07–9.45 GHz) circularly polarized/ > -10 dB (1.0–2.86 GHz, 3.48–4.80 GHz, 5.36–6.05 GHz and 6.91–8.49 GHz) linearly polarized
Miniaturization	16.38% concerning Reference [31]

8.49 GHz. Feed position shift (off-set fed) results in circular polarization. The axial ratio (AR) plot versus frequency with theta and phi zero degrees of the antenna is shown in Figure 10(a).

3.3.1. Antenna Polarization

The axial ratio plot clears the picture of polarization types. The antenna is linearly polarized at frequencies 1.83 GHz, 3.99 GHz, 5.79 GHz, and 7.82 GHz with axial ratios of 66.35 dB, 52.87 dB, 26.97 dB, and 78.12 dB, respectively. The antenna behaves like a circularly polarized antenna with axial ratios of 1.50 dB and 2.01 dB at frequencies 3.20 GHz and 9.28 GHz, respectively, as depicted in Figure 10(a). For a more detailed understanding, the polarization behavior of the antenna left-hand circular polarization (LHCP) and right-hand circular polarization (LHCP) gain, and polarization ratio

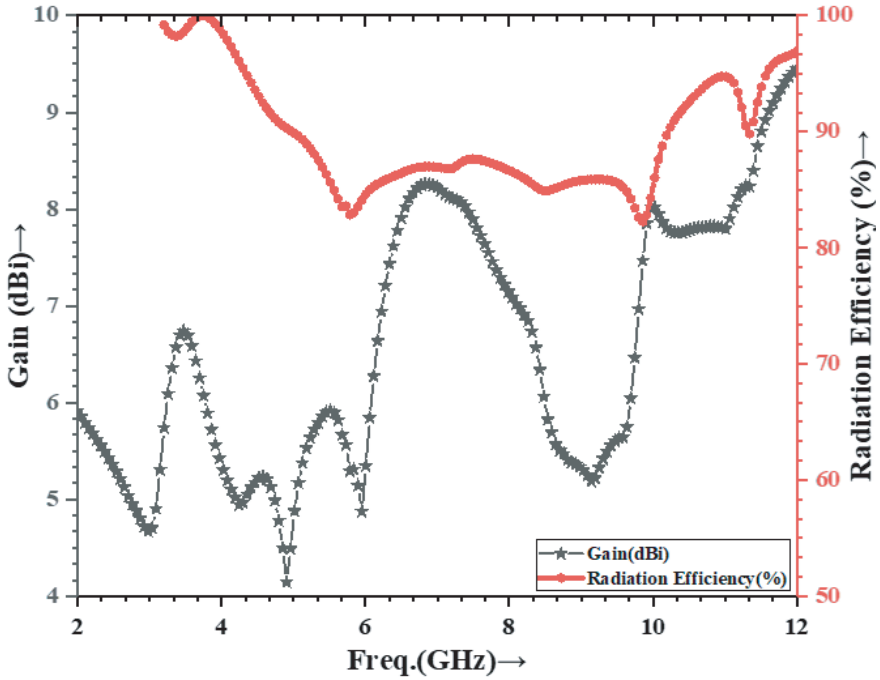

Figure 9. Gain and radiation efficiency plots.

Table 7. Polarization determination of the proposed antenna.

Freq. (GHz)	Gain (dB)		Polarization Ratio (dB)		Gain Comparison	Comment (Type of polarization)
	LHCP	LHCP	LHCP	RHCP		
1.83	0.93	0.89	+0.01	−0.01	LHCP ≈ RHCP	Linearly
3.20	1.23	−20.1	+21.06	−21.06	LHCP > RHCP	Circularly (LHCP)
3.99	−2.20	−2.23	+0.04	−0.04	LHCP ≈ RHCP	Linearly
5.79	−1.79	−2.57	+0.78	−0.78	LHCP ≈ RHCP	Linearly
7.82	−7.22	−7.23	+0.01	−0.01	LHCP ≈ RHCP	Linearly
9.20	−22.30	−3.54	+18.77	−18.77	LHCP < RHCP	Circularly (RHCP)

plots are plotted and analyzed in Figures 10(b) and 10(c), respectively. The polarization behavior of the hybrid fractal UWB antenna is summarized in Table 7.

3.4. Radiation Pattern Plots of Hybrid Fractal Slotted Antenna

The E-plane and H-plane gain radiation plots of simulated and measured odd symmetric hybrid Koch-Minkowski slotted antenna are shown in Figures 11(a)–(d). The E-plane and H-plane radiation patterns are plotted and compared with the simulated patterns at four resonance frequencies 3.20 GHz, 4.94 GHz, 7.22 GHz, and 10.12 GHz. It is concluded that the measured E-plane and H-plane patterns at the four resonant frequencies are deviated from the simulated E-plane and H-plane radiation patterns. The main cause of these deviated radiation patterns might be the power measuring errors or instrumentation errors, some fabrication errors, soldering of the SMA connector at the exact location, or the small variations in the overall substrate dimensions. The 3D-Gain radiation patterns at all four resonance frequencies are shown in Figures 12(a)–(d).

3.5. Selection of Patch Geometry Based on Surface Current Density Distributions

The initial geometry of the Patch is calculated using the standard rectangular patch antenna design equations. A combination of double Minkowski and double Koch slots has been inserted at the bottom edges of the antenna. This will change the electric field and current distribution inside the patch. The electrical lengths fall across the current distribution resulting in a new tuning frequency. Therefore, we can say that slot size length and placing results in the top geometry of the patch.

The surface current density distributions are shown at four resonance frequencies in Figure 13. At the first resonance frequency, the most current is concentrated around the Koch-Koch arms as

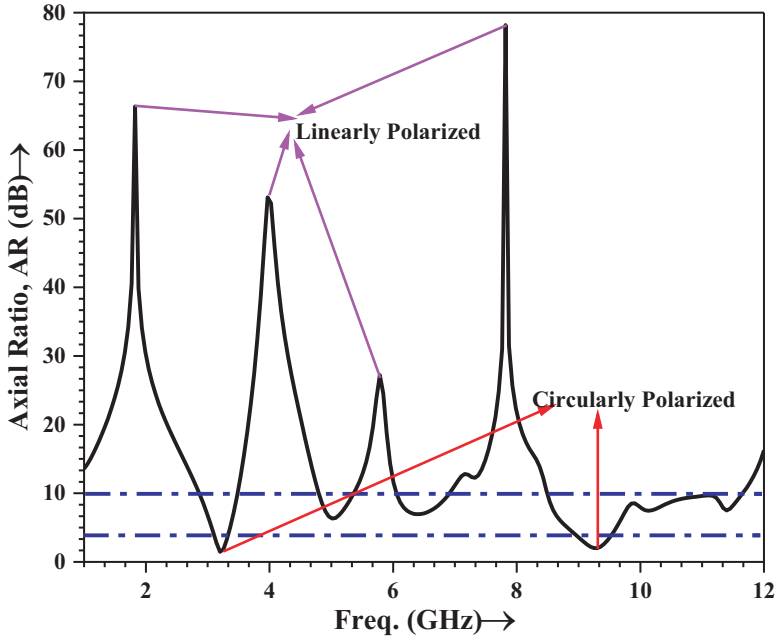

(a)

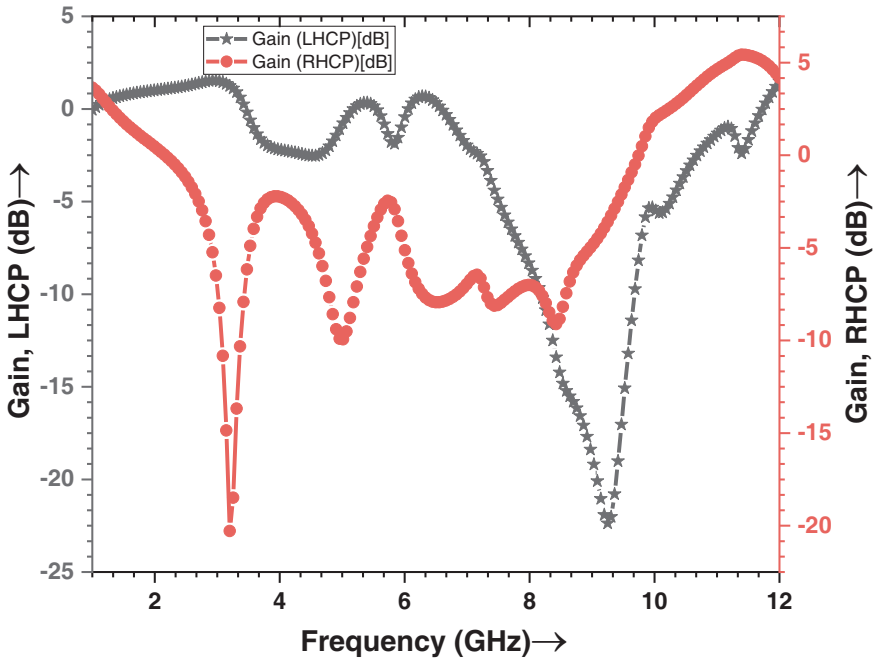

(b)

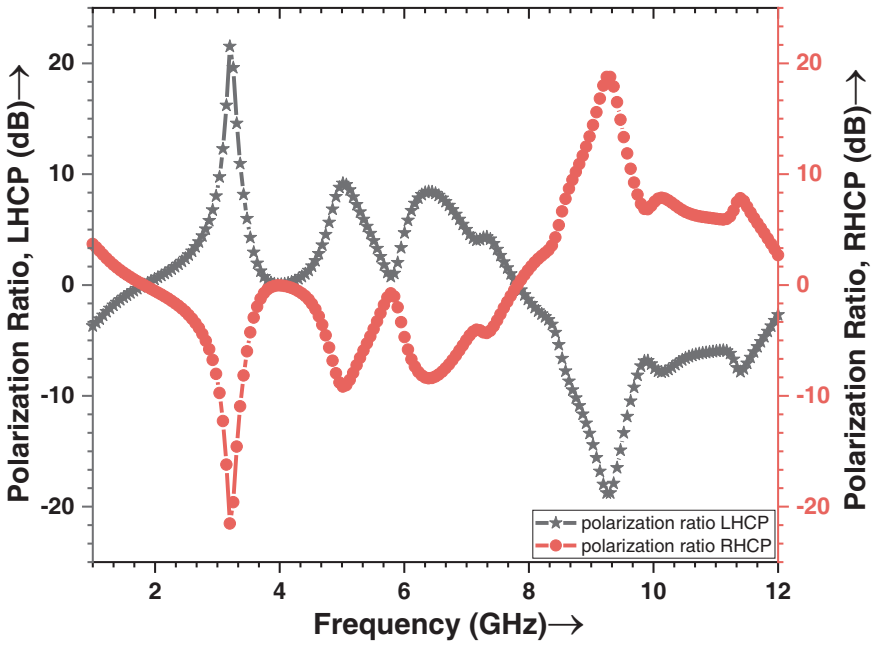

(c)

Figure 10. (a) Axial ratio plots. (b) Left hand and right hand circularly polarized gain plots. (c) Polarization ratio plots.

shown in Figure 13(a). The total electrical length across the current distribution arms is 29.005 mm ($L = a + b + c + d + l + k + j + i$). This results in a resonance tuning frequency of 3.147 GHz, which is nearly equal to 3.20 GHz. Mathematically, tuning frequency is given by

$$f_r = \frac{c}{2L\sqrt{\frac{\varepsilon_r+1}{2}}} \tag{1}$$

where 'L' is the current distribution electrical length.

The second tuning frequency is obtained because of the lower Minkowski and upper Koch arms as shown in Figure 13(b). The total electrical length around this current path is 17.775 mm ($L = f + j + k + i$). Using Equation (1) the evaluated tuning frequency is 5.137 GHz which is approximately close to the 4.94 GHz simulated resonance frequency. At the third resonance frequency, the current is concentrated around the upper Minkowski and lower Koch arms as shown in Figure 13(c). The total electrical length across this path is 12.1725 mm ($L = n + \frac{1}{2}(l + c)$). This results in a tuning frequency of 7.499 GHz, i.e., near the third resonance frequency of 7.22 GHz. Similarly, at the fourth resonance frequency, the current is concentrated around the lower Minkowski arms as shown in Figure 13(d). The vertical arms currents of Minkowski cancel out the effect of each other because of opposite direction flows. Thus the total electrical length across this path is 9.07 mm ($L = a + f + \frac{h}{2}$). This results in a tuning frequency of 10.064 GHz, i.e., near the third resonance frequency of 10.12 GHz.

3.6. Performance Comparison of Proposed Antenna with Similar Existing Antennas

Sharma and Sharma have proposed two transformers edge-fed rectangular patch antennas with a size of $45 \times 38.92\,\text{mm}^2$ using single Koch-Koch and Minkowski-Minkowski fractal slots. Both antennas are dual bands in nature with one narrowband and another wideband [32]. Other fractal slotted antennas using tri-rectangular arms fan-shaped, Mickey-Mouse ear shaped circular fractal slot, Log-periodic using nine square fractal slots, double separate Koch slot fractal, double separate T-Shaped fractal slots, double U-shaped fractal slots have been designed and developed by researchers for multi-band applications [13, 20, 21, 24, 25, 32]. The proposed antenna is better concerning all in terms of

Table 8. Performance comparison of the proposed antenna with existing literature.

Ref.	Substrate (Feeding type)	Hybrid Fractal Slot	Size (mm^2)	Res. Freq. (GHz)	−10 dB BW	FBW (%)	Gain (dBi)
[13] 2015	Roger RO4003 ε_r= 3.55 h = (1.524 +1.524) mm $\tan\delta$ = 0.0021 Proximity fed	9-Square fractal Log-Periodic	173 × 70	3.2/3.6, 3.95/4.2, 4.55, 5.0/ 5.5/6.52/ 7.2, 7.8, 8.3, 10.2, 10.9	3.1–3.3 3.5–4.1 4.2–5.1 5.2–5.8 6.2–6.75 6.9–11.0	6.25 15.78 19.35 10.9 8.5 45.81	11.15 @5 GHz
[20] 2019	Rogers RT Duroid 5880 substrate ε_r = 2.2, $\tan\delta$ = 0.0009 h = 0.508 mm (Inset fed)	Double Separate T-Shaped Slots	20 × 16.5	10/28/38	9–11 27–29 37–39	20 7.14 5.26	5.82 11.48 11.72
[21] 2013	(Coaxial fed)	Double U-shaped slots	50 × 50	3.6/5.2	3.49–3.74 4.92–5.42	7.5 9.6	8.5 8.6
[22] 2017	FR-4 ε_r= 4.4 h = 1.6 mm $\tan\delta$ = 0.02 (Inset fed)	5Rectangule+ 5Circule slots	55 × 35.5	2.81/5.81/7.81, 8.0/8.72	2.79–2.98 5.68–5.9 7.65–8.2 8.6–9.0	1.4/ 1.5/ 1.3, 1.2/ 1.2	3.22/ 4.68/ 5.94, 8.09/ 11.45
[24] 2021	Rogers RT Duroid 5880 substrate ε_r = 2.2, $\tan\delta$ = 0.0009 h = 1.57 mm (Edge fed)	Ear shaped circular	40 × 45	7.4, 11.8, 17.2,20.2, 24.8, 30.3, 38.6	1.22–47.5	190	Varies between 0.2 to 9.7
[25] 2021	FR-4 ε_r= 4.4 h = 1.6 mm $\tan\delta$ = 0.02 (Edge fed)	Added Tri-Rectangular Arms fractals	66.4 × 66.4	2.45	1.81–3.0	48.98	7.16
[31] 2019	FR-4 h = 1.5 mm f_0 = 2.4 GHz $\tan\delta$ = 0.02 (Inset Fed)	Double separate Koch slots	37.29 × 29.06	2.4/4.48/7.57, 8.0/9.4	2.3–2.45 4.4–4.6 7.3–8.1 9.2–9.7	6.25 4.46 10.38 5.31	5.71 dBi @2.37 GHz
[32] 2018	FR-4 ε_r= 4.4 h = 1.6 mm $\tan\delta$ = 0.02 (Transformer fed)	Single Koch-Koch	45×38.92	2.77/8.38	2.51–2.90 7.74–10	14.07 26.96	3.72/7.77
	FR-4 ε_r= 4.4 h = 1.6 mm (Transformer fed)	Single Koch-Minkowski	45×38.92	2.46/8.34	2.38–2.58 7.56–10	8.13 29.25	5.73/5.62
This Work	FR-4 ε_r= 4.4 h = 1.6 mm $\tan\delta$ = 0.02 (Off-set fed)	Double Mixed Koch-Minkowski	38.42 × 38.12	3.20/4.94/ 7.22/10.12	2.85–11.32	119.548	4.72 @3.2 GHz

Table 9. The novelty of the proposed antenna with reference antenna [32].

Based on	Parameter	Reference antenna [32]	Novelty in This work	Achievements
Antenna Geometry	Antenna type	Microstrip patch antenna	Monopole antenna	———
	Feeding technique	Quarter wave impedance transformer fed	Off-Set Edge fed	Better impedance matching in terms of better reflection coefficient (lowest $S_{11} = -42$ dB)
	Fractal curves used	Single-single Hybrid fractal curve combination of Koch-Minkowski	Double-double Hybrid fractal curves combination of Koch-Minkowski (Odd-symmetric)	More Advanced Curve
	Slot position in the patch	MPA with Koch-Minkowski slot placed exactly in the middle.	Monopole antenna with Koch-Minkowski slot placed below lower middle section in the patch	More space as Low ground area for fabrication area of additional electronic components
	Ground	Complete ground	Partial flitted corner ground	Reduced Ground size
Result Performance	Minimum Reflection Coefficient, S_{11} (dB)	−18 dB	−42.02 dB	S_{11} has been improved
	FBW	14.7% (2.41–2.82), 29.26% (7.56–10)	120% (2.85–11.32)	Enhanced BW (8.47 GHz)
	Application Covered/ Resonance Frequencies (GHz)	Dual tuned (2.79 and 8.34 (6.67–10))	Quad tuned (3.2, 4.94, 7.22, and 10.22)	More number of applications covered
	No. of the frequency band	Dual (One narrowband and one wide band)	Single (UWB)	UWB band with respect to NB and WB
	Peak Antenna Gain (dB)	5.73/5.62	6.30	0.68 dB antenna gain Enhancement
	Radiation pattern	Bidirectional (with a lower Front to back ratio)	Bidirectional (with better Front to back ratio)	One-sided antenna gain improved
	Polarization	Linear	Dual-polarized (linear as well as circular)	Dual-polarization achieved
Antenna Size Miniaturization	On size (mm^3)	$45 \times 38.92 \times 1.6$	Compact with $38.12 \times 38.42 \times 1.6$	16.38%

performance parameters as it has a UWB fractional bandwidth of 119.58%, quad-tuned frequency, and a miniaturized size of $38.12 \times 38.42\,\text{mm}^2$. Therefore, a total of 16.38% size miniaturization has been achieved concerning the base antenna [32] with off-set fed odd-symmetric mixed hybrid double Koch-Minkowski fractal slot of width 0.5 mm. The performance parameters of the proposed odd-symmetric hybrid fractal Koch-Minkowski antenna comparison with similarly existing antennas are arranged in Table 8.

3.7. Novelty of Proposed Antenna Concerning Reference Antenna [32]

The proposed antenna has several novelties concerning reference design antenna [32]. The proposed antenna and reference antenna were designed at the same frequency of 3.2 GHz, but the 16.38% size miniaturization has been achieved in the proposed work. Therefore, the proposed antenna is compact in size. In the proposed antenna a double Koch-Minkowski hybrid slot is placed at the lower middle section where the current density magnitude had minimum values. On the other hand, in the reference

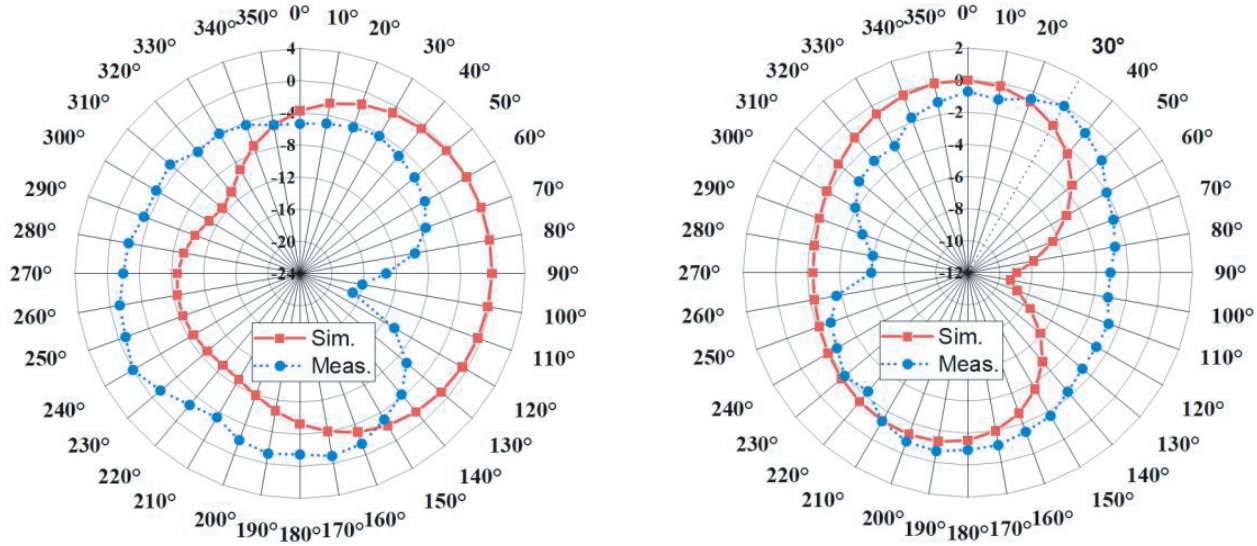

(i) *E*-Plane (ii) *H*-Plane

(a)

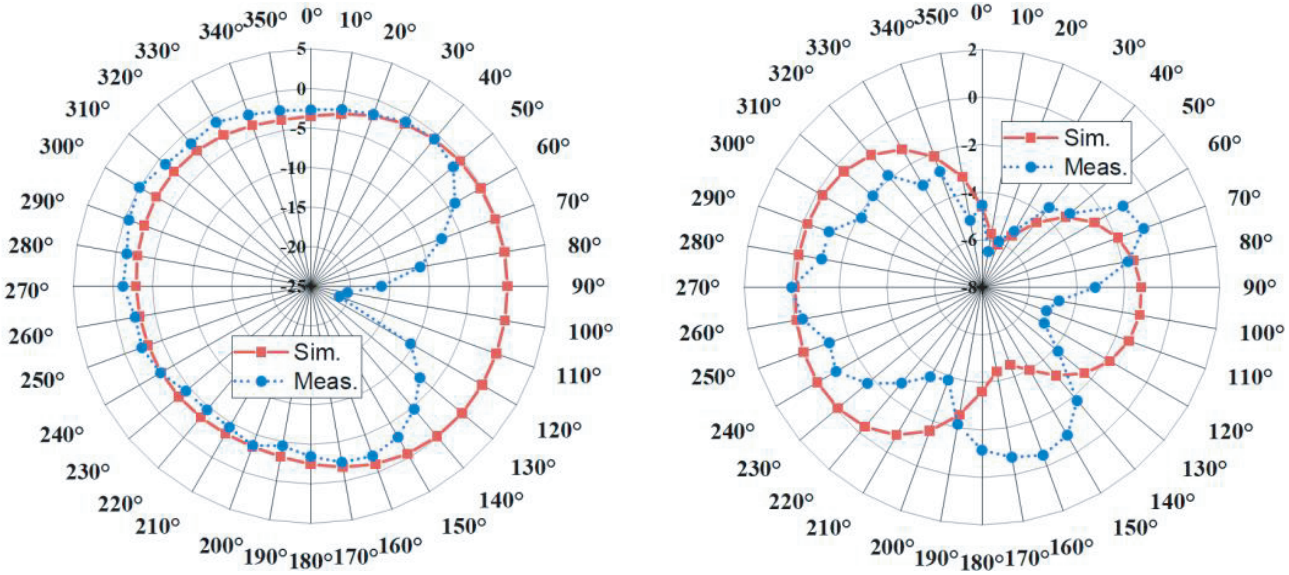

(i) *E*-Plane (ii) *H*-Plane

(b)

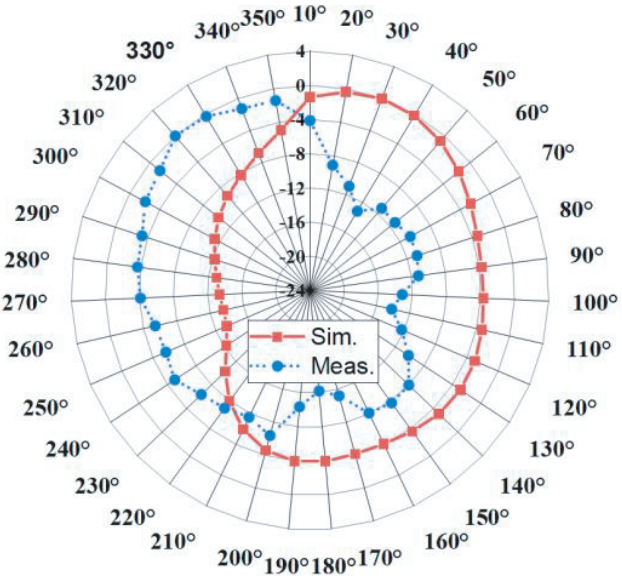

(i) *E*-Plane

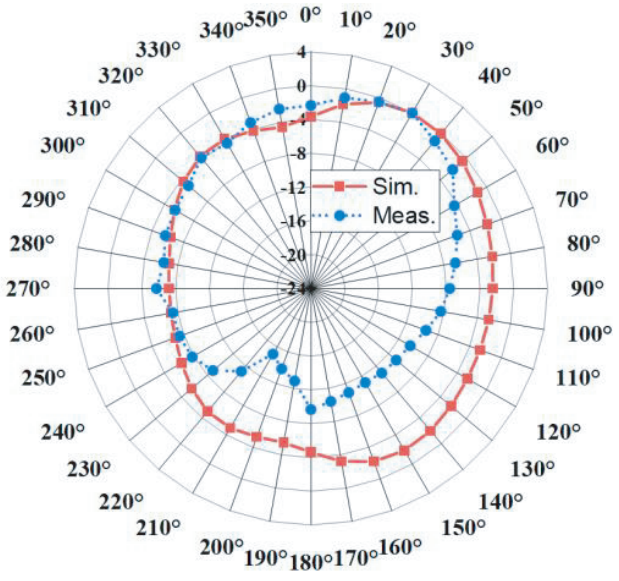

(ii) *H*-Plane

(c)

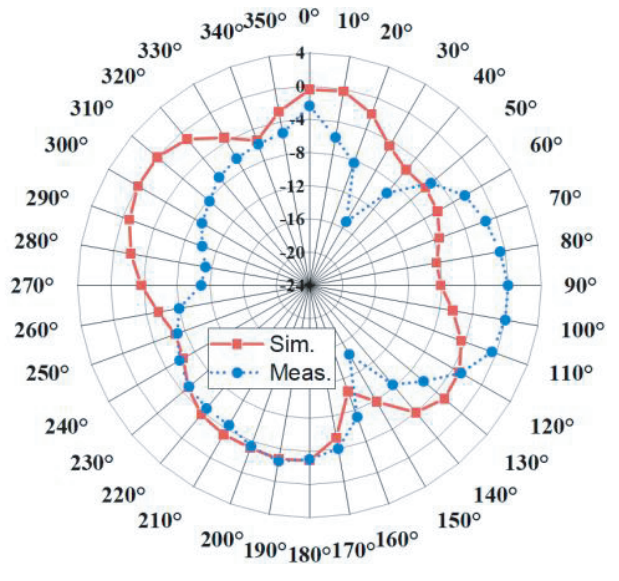

(i) *E*-Plane

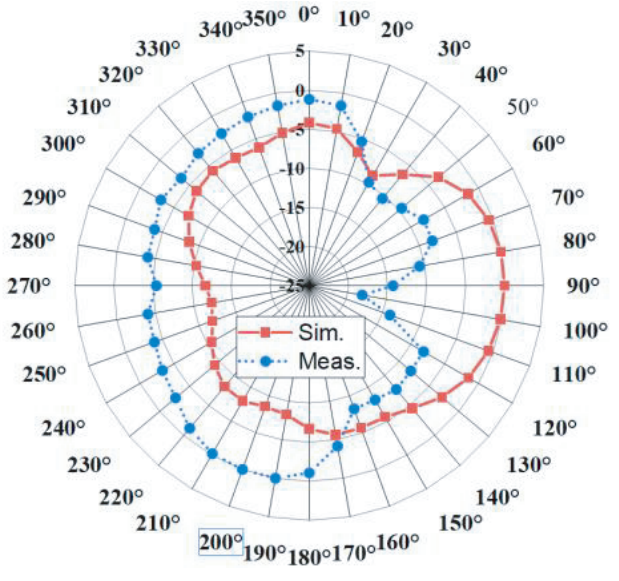

(ii) *H*-Plane

(d)

Figure 11. Radiation patterns. (a) @ $f_{r1} = 3.20\,\text{GHz}$. (b) @ $f_{r2} = 4.94\,\text{GHz}$. (c) @ $f_{r3} = 7.22\,\text{GHz}$. (d) @ $f_{r4} = 10.12\,\text{GHz}$.

antenna, a single Koch-Minkowski hybrid slot is placed exactly in the middle without concern about current density distribution magnitude values. The placing of the hybrid slot at the right location results in UWB applications [26] whereas the reference antenna was proposed and designed for wideband applications [dual widebands]. The proposed designed antenna is good in terms of enhanced fractional BW (120%), minimum reflection coefficient (−42.02 dB), of course, improved VSWR values. The offset feeding technique is used instead of the normally used edge-feed or impedance transformer feed results in not only a better reflection coefficient but also dual polarizations and peak gain enhancement of 0.68 dB at a frequency of 10.22 GHz. Concerning the radiation pattern point view, the proposed

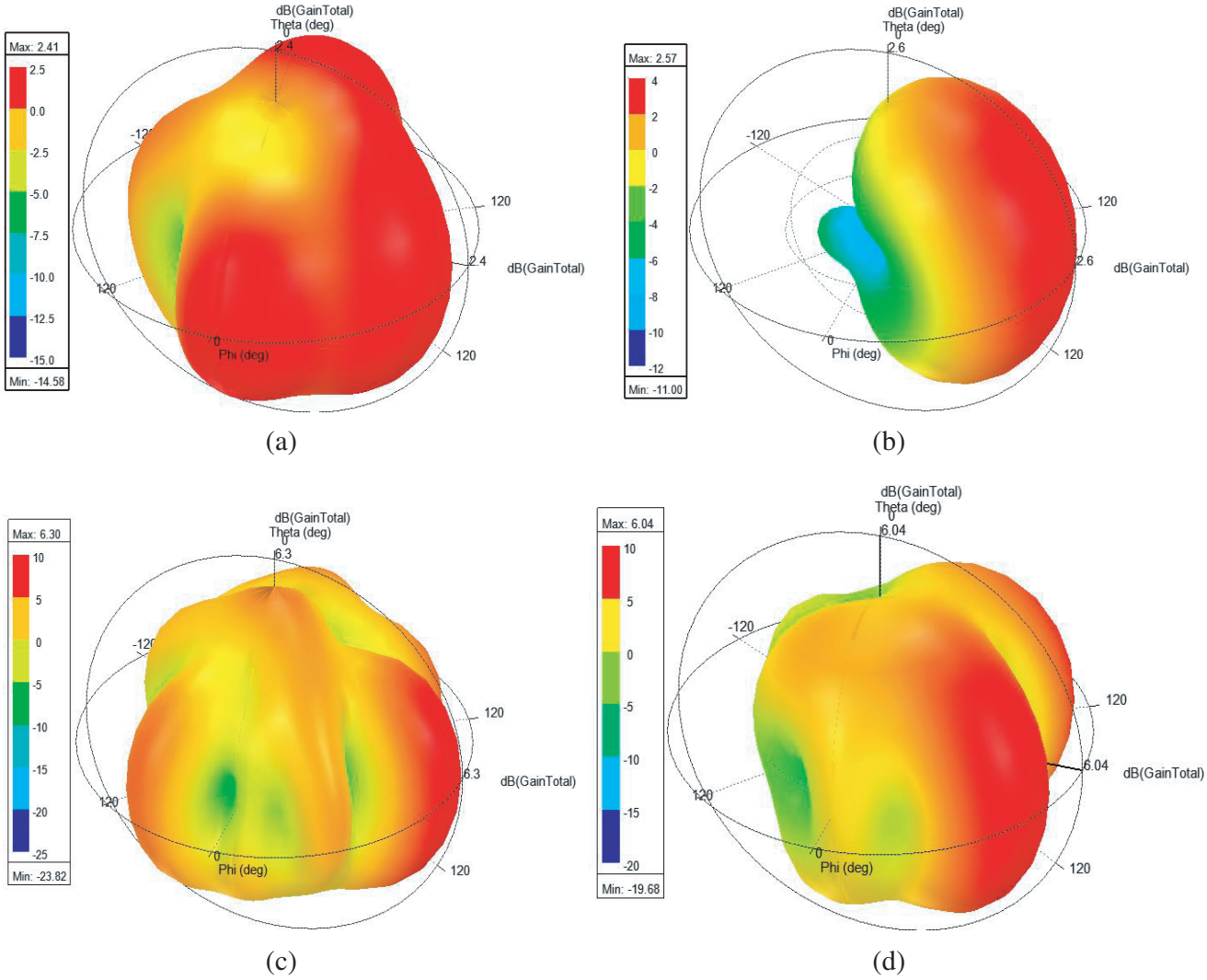

Figure 12. 3D-radiation patterns. (a) @3.20 GHz. (b) @4.94 GHz. (c) @7.22 GHz. (d) @10.12 GHz.

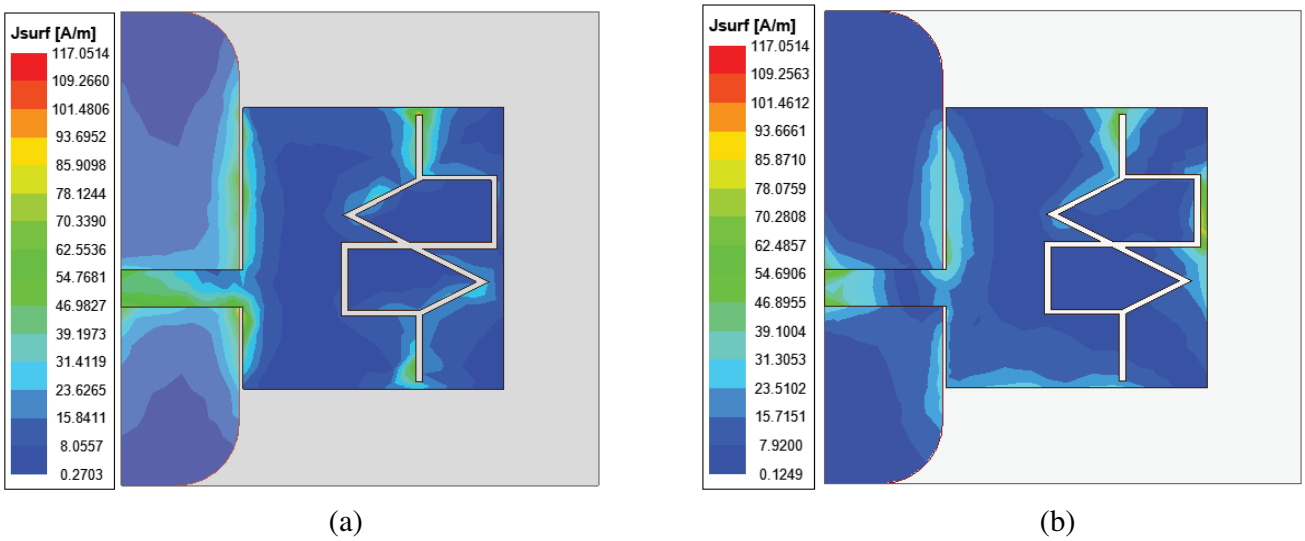

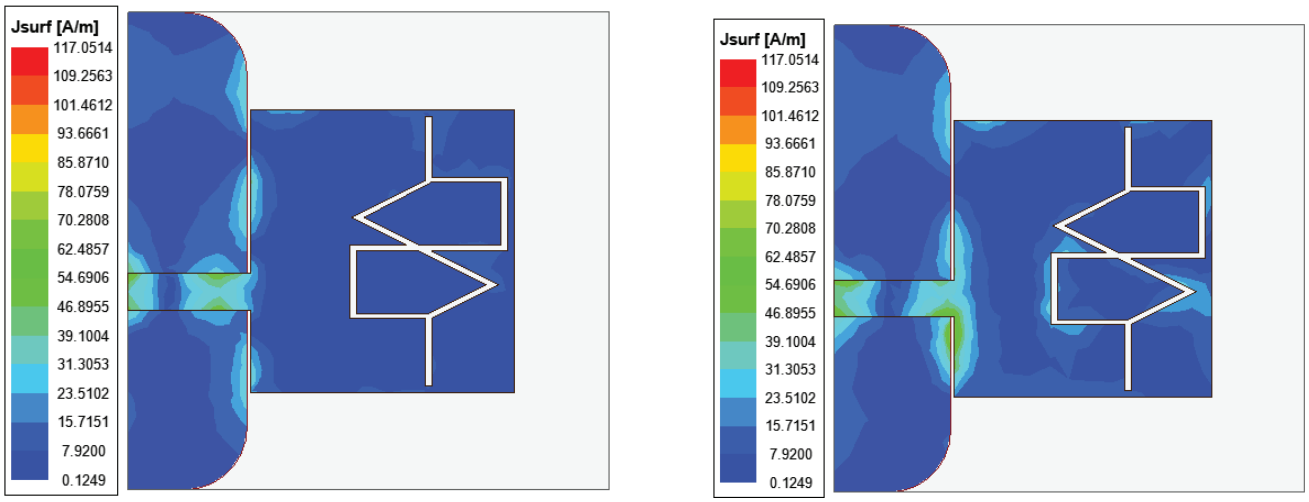

Figure 13. Surface current Distribution on the proposed antenna shows four resonances. (a) @3.20 GHz. (b) @4.94 GHz. (c) @7.22 GHz. (d) @10.12 GHz.

antenna has a better front-to-back lobe ratio (FBR) than the reference antenna and hence results in improved gain performance in one direction at a frequency of 10.22 GHz. The novelty of the proposed antenna prototype concerning reference antenna is provided in Table 9.

4. CONCLUSIONS

An off-set fed odd-symmetric hybrid fractal double mixed Minkowski-Koch slotted rectangular monopole UWB antenna is fabricated, tested, and analyzed. The fabricated antenna is economical since a low-profile piece of FR-4 substrate has been utilized with dimensions $0.741\lambda_g \times 0.747\lambda_g$. Guided wavelength, λ_g, was calculated at a design frequency of 3.2 GHz. The measured and simulated results are found to concord with each other in shape with small considerable deviations in the four resonance frequencies within the measured UWB 2.11–11.73 GHz span. The antenna is dual polarized, circular and linear with AR < -3 dB and AR > -3 dB, respectively. The proposed antenna has a peak gain of 8.3 dBi at a frequency of 7.10 GHz and 4.72 dBi at a design frequency of 3.20 GHz with a peak radiation efficiency of 89.81% achieved. The simulated and measured radiation patterns are in tiny worsening with each other at four tuning 3.2 GHz, 4.94 GHz, 7.22 GHz, and 10.12 GHz frequencies. The designed antenna using an FR-4 substrate exhibits high gain values (> 8 dBi) at frequencies above 9 GHz and good gain value (> 6 dBi) between frequencies 6 GHz and 9 GHz also. The proposed antenna with approximate UWB fractional bandwidth of 139 % is a suitable candidate for WiFi, WLAN, PCS, WiMAX, Sub-6 GHz, and Satellite, Radar, military, space research, satellite-fixed mobile, S-band, C-band, and X-band applications. In the future, the proposed antenna could be modified to be frequency reconfigurable using PIN diodes, polarization reconfigurable, and pattern reconfigurable using varactor diode, and because of compactness the proposed antenna could be used for MIMO system for high data rate and diversity resolution.

ACKNOWLEDGMENT

This project has received funding from the European Union's Horizon 2020 research and innovation program under grant agreement H2020-MSCA-RISE-2018-EXPLOR-872897. This work is also funded by the FCT/MEC through national funds and when applicable co-financed by the ERDF, under the PT2020 Partnership Agreement under the UID/EEA/50008/2020 project.

REFERENCES

1. Azim, R. and M. T. Islam, "Compact planar UWB antenna with band notch characteristics for WLAN and DSRC," *Progress In Electromagnetics Research*, Vol. 133, 391–406, 2013.
2. Syed, A. and R. W. Aldhaheri, "A very compact and low profile UWB planar antenna with WLAN band rejection," *The Sci. World J.*, Vol. 7, 1–7, 2016.
3. Gianvittorio, J. P. and Y. R. Samii, "Fractal antennas, a novel antenna miniaturization technique, and applications. *IEEE Ants. and Propaga. Mag.*, Vol. 44, No. 1, 20–36, 2002.
4. Werner, D. H. and S. Ganguly, "An overview of fractal antenna engineering research," *IEEE Ants. and Propag. Mag.*, Vol. 45, No. 1, 38–57, 2003.
5. Mirzapour, B. and H. R. Hassani, "Size reduction and bandwidth enhancement of snowflake fractal antenna," *IET Microw., Ants. & Propag.*, Vol. 2, No. 2, 180–187, 2008.
6. Park, J. K., H. S. An, and J. N. Lee, "Design of the tree-shaped UWB antenna using a fractal concept. *Microw. and Opt. Tech. Lett.*, Vol. 50, No. 1, 144–150, 2008.
7. Thakare, Y. B. and R. Kumar, "Design of fractal patch antenna for size and radar cross-section reduction," *IET Microw., Ant. & Propag.*, Vol. 4, No. 2, 175–181, 2010.
8. Azari, A., "A new super wideband fractal microstrip antenna," *IEEE Trans. on Ant. and Propag.*, Vol. 59, No. 5, 1724–1727, 2011.
9. Pourahmadazar, J., C. Ghobadi, J. Nourinia, "Novel modified pythagorean tree fractal monopole antennas for UWB applications," *IEEE Ant. and Wirel. Propag. Lett.*, Vol. l, No. 10, 484–487, 2011.
10. Maza, A. R., B. Cook, G. Jabbour, and A. Shamim, "Paper-based inkjet-printed ultra-wideband fractal antennas," *IET Microw. Ants. and Propag.*, Vol. 6, No. 12, 1366–1373, 2012.
11. Fallahi, H. and Z. Atlasbaf, "Study of a class of UWB CPW-fed monopole antenna with fractal elements," *IEEE Ant. and Wirel. Propag. Lett.*, Vol. 12, 1484–1487, 2013.
12. Reddy, V. V. and N. V. S. N. Sharma, "Triband circularly polarized Koch fractal boundary microstrip antenna," *IEEE Ant. and Wirel. Propag. Lett.*, Vol. 13, 1057–1060, 2014.
13. Amini, A. and H. Oraizi, "Miniaturized UWB log-periodic square fractal antenna," *IEEE Ant. and Wirel. Propag. Lett.*, Vol. 14, 1322–1325, 2015.
14. Zhao, Y.-L., Y.-C. Jiao, G. Zhao, L. Zhang, Y. Song, and Z.-B. Wong, "Compact planar monopole UWB antenna with band-notched characteristic," *Microw. and Opt. Tech. Lett.*, Vol. 50, No. 10, 2656–2658, 2008.
15. Liu, H.-W., C.-H. Ku, T.-S. Wang, and C.-F. Yang, "Compact monopole antenna with band-notched characteristic for UWB applications," *IEEE Ant. and Wirel. Propag. Lett.*, Vol. 9, No. 1, 397–400, 2010.
16. Patil, S. and V. Rohokale, "Multiband smart fractal antenna design for converged 5G wireless networks," *International Conference on Pervasive Computing (ICPC)*, 1–5, Pune, 2015.
17. Abdalla, M. A., A. A. Ibrahim, and A. Boutejdar, "Resonator switching techniques for notched ultra-wideband antenna in wireless applications," *IET Microw., Ant. and Propag.*, Vol. 9, No. 13, 1468–1477, 2015.
18. Zarrabia, F. B., Z. Mansourib, N. P. Gandjic, and H. Kuhestanib, "Triple-notch UWB monopole antenna with fractal Koch and T-shaped stub," *AEU — Intern. J. of Electr. and Comm.*, Vol. 70, No. 1, 64–69, 2016.
19. Yadav, A., D. Sethi, and R. K. Khanna, "Slot loaded UWB antenna: Dual band-notched characteristics," *AEU Intern. J. of Electr. and Comm.*, Vol. 70, No. 8, 331–335, 2016.
20. Abdelaziz, A., K. Ehab, and I. Hamad, "Design of a compact high gain microstrip patch antenna for tri-band 5G wireless communication," *Frequenz*, Vol. 73, 45–52, 2018.
21. Liu, S., S. Qi, W. Wu, and D.-G. Fang, "Single-fed dual-band dual-polarized U-slot patch antenna," *IEEE MTT-S International Microwave Workshop Series on RF and Wireless Technologies for Biomedical and Healthcare Applications (IMWS-BIO)*, 2013.

22. Kaur, N. and N. Sharma, "Designing of slotted microstrip patch antenna using Inset Cut line feed for S, C and X-band applications," *Internat. J. of Electr. Engg. R.*, Vol. 9, No. 7, 957–969, 2017.
23. Shimizu, K. and T. Fujimoto. "A printed inverted-F antenna for dual-band dual-sense circular polarization," *IEEE International Workshop on Electromagnetics: Applications and Student Innovation Competition (iWEM)*, 1–1, August 2018.
24. Varshney, A., T. M. Neebha, V. Sharma, J. Grace, and A. Diana, "Dodecagon-shaped frequency reconfigurable antenna practically loaded with 3-Delta structures for ISM band and wireless applications," *IETE Journal of Research*, 1–13, 2022.
25. Varshney, A., N. Cholake, and V. Sharma, "Low-cost ELC-UWB fan-shaped antenna using parasitic SRR triplet for ISM band and PCS applications," *Inter. J. of Electr. Lett.*, Vol. 10, No. 4, 391–402, 2021.
26. Kshetrimayum, R. S., "An introduction to UWB communication systems," *IEEE Potentials*, Vol. 28, No. 2, 9–13, 2009.
27. Ali, T., B. K. Subhash, S. Pathan, and R. C. Biradar, "A compact decagonal-shaped UWB monopole planar antenna with the truncated ground plane," *Microw. Opt. Technol. Lett.*, Vol. 60, 2937–2944, 2018.
28. Verma, I., P. Singh, H. Kumar, and M. R. Tripathy, "Maple leaf planar fractal antenna for energy harvesting applications," *Proceeding of the International Conference on Intelligent Communication, Control, and Devices, of the Series Advances in Intelligent Systems and Computing*, Vol. 479, 919–925, 2016.
29. Swedheetha, C., M. Suganya, P. Gunapandian, and B. Manimegalai, "Minkowski fractal based antenna for cognitive radio," *IEEE Intern. Micro and RF Conf. (IMaRC)*, 166–169, Bangalore, 2014.
30. Wei, K., J. Y. Li, L. Wang, Z. J. Xing, and R. Xu, "Mutual coupling reduction by novel fractal defected ground structure bandgap filter," *IEEE Trans. on Ant. and Propag.*, Vol. 64, No. 10, 4328–4335, 2016.
31. Fonseca, D., F. Pereira, Ulysses, and R. C. Vitor, "Study of patch antennas with koch curve form slots," *J. of Microw., Optoelectr. and Electromag. Appl.*, Vol. 18, 399–407, 2019.
32. Sharma, N. and V. Sharma, "A design of microstrip patch antenna using hybrid fractal slot for wideband applications," *Ain. Shams. Engineering Journal*, Vol. 9, 2491–2497, 2018.
33. Tizyi, H., F. Riouch, A. Tribak, A. Najid, and A. M. Sanchez, "CPW and microstrip line-fed compact fractal antenna for UWB-RFID applications," *Progress In Electromagnetics Research C*, Vol. 65, 201–209, 2016.
34. Ladhar, L., M. Zarouan, D. Oueslati, J.-M. Floch, and H. Rmili, "Investigation on cellular-automata irregular-fractal ultra wideband slot-antennas," *Microw. and Optic. Tech. Lett.*, Vol. 57, No. 11, 2506–2514, 2015.
35. Kim, G. and S. Kim, "Design, and analysis of dual polarized broadband microstrip patch antenna for 5G mm-wave antenna module on FR4 substrate," *IEEE Access*, Vol. 9, 64306–64316, 2021.